A photoproduct of DXCF cyanobacteriochromes without reversible Cys ligation is destabilized by rotating ring twist of the chromophore

Title

Photoproduct of DXCF cyanobacteriochromes without reversible Cys ligation is destabilized by rotating ring twist of the chromophore

Keiji Fushimi[a,b], Takumi Matsunaga[a], Rei Narikawa[a,b,c,1]

[a]Department of Biological Sciences, Faculty of Science, Shizuoka University, 836 Ohya, Suruga, Shizuoka 422-8529, Japan

[b]Core Research for Evolutional Science and Technology, Japan Science and Technology Agency, 4-1-8 Honcho, Kawaguchi, Saitama 332-0012, Japan

[c]Research Institute of Green Science and Technology, Shizuoka University, 836 Ohya, Suruga, Shizuoka 422-8529, Japan

[1]To whom correspondence should be addressed.

Email: narikawa.rei@shizuoka.ac.jp, Tel: +81-54-238-4783

Abstract

Cyanobacteriochrome photoreceptors (CBCRs) ligate linear tetrapyrrole chromophore via its first (canonical) Cys residue and show reversible photoconversion triggered by light-dependent *Z*/*E* isomerization of the chromophore. Among the huge repertoire of the CBCRs, DXCF CBCRs contain a second Cys residue within the highly conserved Asp-Xaa-Cys-Phe (DXCF) motif. In the typical receptors, the second Cys covalently attaches to the 15*Z*–chromophore in the dark state and detaches from the 15*E*–chromophore in the photoproduct state, whereas atypical ones that lack reversible ligation activity show red-shifted absorption in the dark state due to more extended π-conjugated system. Moreover, some DXCF CBCRs show blue-shifted absorption in the photoproduct state due to the twisted geometry of the rotating ring. During the process of rational color tuning of a certain DXCF CBCR, we unexpectedly found that twisted photoproducts of some variant molecules showed dark reversion to the dark state, which prompted us to hypothesize that the photoproduct is destabilized by twisted geometry of the rotating ring. In this study, we comprehensively examined the photoproduct stability of twisted and relaxed molecules derived from the same CBCR scaffolds under the dark condition. In the DXCF CBCRs lacking reversible ligation activity, the twisted photoproducts showed faster dark reversion than the relaxed ones, supporting our hypothesis. By contrast, in the DXCF CBCRs with reversible ligation activity, the twisted photoproducts showed no detectable photoconversion. Reversible Cys adduct formation thus results in drastic rearrangement of the protein–chromophore interaction in the photoproduct state, which would contribute to the previously unknown photoproduct stability.

Introduction

Cyanobacteriochrome photoreceptors (CBCRs), found only in cyanobacteria, belong to a photoreceptor superfamily that includes linear tetrapyrrole chromophores (or bilin pigments), such as phycocyanobilin (PCB) and phycoviolobilin (PVB). The range of light wavelength absorbed by the CBCRs is determined by the effective length of the π-conjugated system in the chromophores. This length depends on binding chromophore species and protein–chromophore interaction.[1–25] CBCRs are covalently bound to C3[1] position of the chromophore via highly conserved "first" (or "canonical") Cys residue[26–29] similar to the related plant-type phytochromes (Figs. 1A–D and S1A, B).[30–32] They show reversible photoconversion triggered by light-dependent *Z*/*E* isomerization of a double bond between C15–C16 in the chromophore (Figs. 1A–D and S1A, B). A huge repertoire of CBCRs showing photoreaction in a wide range of wavelength has been identified[33,34] and characterized in detail.[26–29,35]

CBCRs are categorized into many subfamilies, with many of them applying "second" (or "DXCF") Cys residue in the highly conserved Asp-Xaa-Cys-Phe (DXCF) motif as a crucial color tuner possessing a dual role, i.e., isomerization activity from PCB to PVB and reversible ligation activity to the chromophore. Typical molecules such as TePixJg retain the dual role and show blue/green photocycle (Fig. 1A, B, E and S1A, B).[11,26,28,36] They initially incorporate PCB as a precursor and then isomerize it to PVB.[37] Moreover, the second Cys covalently attaches to C10 position in the dark state (or ground state) and detaches in the photoproduct state (or excited state), reversibly altering effective length of the π-conjugated system between C-to-D (Fig. 1A, E and S1A) and B-to-D (Fig. 1B, E, and S1B) rings that absorb blue and green light, respectively. Besides, atypical DXCF CBCRs lacking one of the two roles have been reported; CBCRs lacking the isomerization activity absorb red-shifted yellow-to-orange light in the photoproduct state by PCB incorporation (Fig. S2A-i)[7,12,18,21],

whereas the other ones lacking the ligation activity absorb green-to-yellow light in the dark state without π-conjugation cleavage at C10 position (Fig. 1C, E, and S2A-ii).[3,7,18,24,38] The first Cys covalently attaches to the $C3^1$ position in any case (Figs. 1A–D and S1A, B). The lack of the second Cys ligation activity is caused by replacement of Tyr residue with His next to the first Cys (Fig. S2A-iii).[38]

In addition, some DXCF CBCRs adopt a unique color tuning mechanism, "trapped-twist" in which twisted geometry of ring D results in blue-shifted teal light absorption in the photoproduct state in comparison with those of the typical ones (Fig. 1D, E and Fig. S2A-iv)[3,7,18,24,38] This mechanism has been well supported by theoretical and experimental evidences based on the chromophore chemistry.[19] The twisted ring D is held by specific Phe residue(s) on a β–sheet with or without an α–helix, and replacement of these residues results in cancellation of the twisted geometry (Figs. 1D, F, and S2A-iv, B).[38,39] We have further reported that not only the twisted photoproduct state but also the twisted dark state contribute to additional color tuning, for which two residues near the ring D (Tyr/Leu and Thr/Asn positions) are crucial (Fig. S2A-ii).[38]

Taken together, the spectral diversity of the DXCF CBCRs can be explained by various combinations of four mechanisms: PCB-to-PVB isomerization activity, second Cys ligation activity, and regulation of the ring D geometry in the dark state and the photoproduct state (Fig. S2A).[38]

Recently, we have identified a unique molecule, AM1_1499g1, which belongs to the DXCF subfamily but has lost the second Cys (Fig. S2B).[38] By comparing it with related molecules retaining the second Cys, we have successfully identified residues crucial for each color tuning mechanism and created seven color-tuned variants with a broad wavelength range derived from a single CBCR scaffold.[38]

During the engineering process, we unexpectedly found that the "trapped-twist" photoproduct states of some variant molecules showed dark reversion to the dark state. Dark reversion kinetics presumably is associated with the stability of ring D of 15*E*–chromophore in the photoproduct state. Therefore, it is likely that the twisted ring D is less thermodynamically stable than the relaxed one. To date, only rare DXCF CBCRs with unique sequence arrangement have been reported to show dark reversion.[5,7]

In this study, to gain insights into general characteristics of dark reversion of the DXCF CBCRs, we compared dark reversion kinetics of the relaxed and twisted photoproduct states derived from the same CBCR scaffolds. We found that the twisted photoproduct states showed faster dark reversion than the relaxed ones, except for the molecules showing reversible Cys adduct formation, in which both twisted and relaxed photoproduct states were stable under the dark condition. Possible mechanisms underlying these phenomena are discussed in the context of molecular structure.

Experimental

Bacterial strains and growth media

The *Escherichia coli* strain Mach1 $T1^R$ (Thermo Fisher Scientific) was used during cloning of plasmids. The *E. coli* strain C41 (Cosmo Bio) was used for protein expression through the pKT271 construct as a PCB synthetic system.[40,41] Bacterial cells were grown on Lysogeny Broth (LB) agar medium containing 20 μg mL^{-1} kanamycin with or without 20 μg mL^{-1} chloramphenicol at 37°C. For protein expression, after the optical density at 600 nm of the cells reached 0.4–0.8, isopropyl β-D-1-thiogalactopyranoside was added (final concentration, 0.1 mM), and the cells were cultured at 18°C overnight before being harvested.

Bioinformatic analysis.

Multiple sequence alignment and neighbor-joining phylogenetic trees were constructed using MEGA7 software.[42] Structural information (^{15Z}Pb_TePixJg, PDB_ID: 4GLQ[26]; ^{15E}Pg_TePixJg, PDB_ID: 3VV4[28]; and ^{15E}Pg_Slr1393g3, PDB_ID: 5M82[29]) were extracted from databases and used to compare conformation near the chromophores. Images of molecular structure were generated by UCSF Chimera software.[43]

Plasmid construction for protein expression

The plasmids of AM1_1499g1 (amino acid positions 47–222), AM1_6305g1 (amino acid positions 33–203), and AM1_0048g1 (amino acid positions 199–366) variants were constructed from their corresponding parent plasmids, which were constituted by insertion of their corresponding gene fragments fused with N-terminal His-tag sequence into the pET28a vector (Novagen).[7,38] The plasmids of AM1_1499g1_$S_{118}C$, $S_{118}C/Y_{151}L/T_{159}N$, $S_{118}C/H_{147}Y$, $F_{97}V/S_{118}C$, $F_{97}V/S_{118}C/Y_{151}L/T_{159}N$, and $F_{97}V/S_{118}C/H_{147}Y$, and AM1_6305g1_$L_{132}Y/N_{140}T$ variants have been constructed in the previous study.[38] The plasmids of AM1_6305g1_$F_{78}V$

and $F_{78}V/L_{132}Y/N_{140}T$, and AM1_0048g1_$F_{241}V/F_{298}L$ were generated by site-directed mutagenesis using corresponding parent plasmids. KOD One PCR Master Mix (Toyobo Life Science) with appropriate nucleotide primer sets (AM1_6305g1, forward primer 5′-GGATGCgtcGTTGCTGAAAAAGTAGTTCCG-3′ and reverse primer 5′-AGCAACgacGCATCCCGTTGTATAGTT-3′ for replacement of Phe78 by Val; AM1_0048g1, forward primer 5′-GGTACCgtcGTCGCCGAATCTGTTGCCCC-3′ and reverse primer 5′-GGCGACgacGGTACCCTCACCGTTATTGTTGAGG3′ for replacement of Phe241 by Val, and forward primer 5′-GAGCGTctcGCCGTCAAAGCAAACATT-3′ and reverse primer 5′-GACGGCgagACGCTCTAGCAAACCGAT-3′ for replacement of Phe298 by Leu; each mutation site is shown by small letters) was used for the mutagenesis. Plasmid sequences were confirmed by DNA sequencing (Eurofins Genomics). The plasmid of NpR5113g3 (amino acid positions 388–557) has been constituted in the previous study.[38]

Protein extraction and purification

All proteins were expressed in the *E. coli* strain C41 containing pKT271 in 1 L LB. After expression was induced, the culture broth was centrifuged at 5,000 g for 15 min to collect cells. The cells were resuspended in the lysis buffer (20 mM HEPES–NaOH pH 7.5, 0.1 M NaCl and 10% (w/v) glycerol) with 0.5 mM tris(2-carboxyethyl)phosphine. Protein was purified as described in the previous studies.[7,38] Purified proteins were dialyzed against the lysis buffer containing 1 mM dithiothreitol (DTT). Protein concentration was determined by the Bradford method.

Electrophoresis and fluorescence detection

Purified proteins were diluted in a buffer (60 mM Tris–HCl pH 8.0, 2% (w/v) sodium dodecyl sulfate (SDS) and 60 mM DTT), denatured at 95°C for 3 min, and electrophoresed at

room temperature (r.t.) using 12% (w/v) SDS polyacrylamide gels. The electrophoresed gels were soaked in distilled water for 30 min before fluorescence bands were visualized as previously described.[6,27] Gels were then stained with Coomassie Brilliant Blue R-250.

Spectroscopy and dark reversion kinetics

Ultraviolet and visible absorption spectra of the proteins were recorded with a UV-2600 spectrophotometer (SHIMADZU) at r.t. or 30°C using a thermostated cuvette holder. An Opto-Spectrum Generator (Hamamatsu Photonics, Inc.) was used to generate monochromatic light of various wavelengths to induce photoconversion: Pb form, 390–420 nm; Pt form, 470–490 nm; Pg form, 490–580 nm; Py form, 580–640 nm.

For monitoring dark reversion of CBCRs, the absorbance of photoproduct states and transition process at each maximum absorption of dark states were chronologically measured in the dark condition. The half-life was calculated from the dark reversion kinetics.

Biochemical characterization of cyanobacteriochromes

For denaturation assays, native AM1_6305g1_F_{78}V and F_{78}V/L_{132}Y/N_{140}T, and AM1_0048g1_F_{241}V/F_{298}L in both the dark state (15*Z*–isomer) and photoproduct state (15*E*–isomer) were diluted fivefold in 8 M acidic urea (pH < 2.0). Their absorption spectra were recorded at r.t. before and after 3 min of illumination with white light. Assignment of the chromophore species was conducted by comparing the spectra between native and each denatured molecule which incorporates PVB.[7,38]

Results

Dark reversion of AM1_1499g1 variants

In the previous study, we have created the twisted and relaxed molecules derived from the same AM1_1499g1 scaffold: AM1_1499g1_wild-type (orange/green photocycle), AM1_1499g1_$S_{118}C$ (yellow/teal photocycle), $S_{118}C/Y_{151}L/T_{159}N$ (green/teal photocycle) and $S_{118}C/H_{147}Y$ (blue/teal photocycle) for the twisted type; AM1_1499g1_$F_{97}V$ (orange/yellow photocycle), AM1_1499g1_$F_{97}V/S_{118}C$ (yellow/green photocycle), $F_{97}V/S_{118}C/Y_{151}L/T_{159}N$ (green/green photocycle), and $F_{97}V/S_{118}C/H_{147}Y$ (blue/green photocycle) for the relaxed type.[38] While analyzing spectroscopy of these molecules, we incidentally found that some variant molecules showed dark reversion, which led us to hypothesize that the twisted ones are unstable and tend to show dark reversion in comparison with the relaxed ones. To test this hypothesis, we measured the absorption spectra of the photoproduct states during dark incubation at 30°C to monitor the dark reversion for 5 hours (Fig. 2 and Table 1). We have previously reported that the photoproduct state of AM1_1499g1_wild-type showed thermochromism, which reflects an equilibrium between the twisted state and relaxed state.[38] Therefore, we excluded AM1_1499g1_wild-type and its related AM1_1499g1_$F_{97}V$ from this analysis.

We found that the twisted photoproduct states of AM1_1499g1_$S_{118}C$ and AM1_1499g1_$S_{118}C/Y_{151}L/T_{159}N$ showed dark reversion under the condition described above (at 30ºC for 5 hours) (Fig. 2A, C), whereas the relaxed counterparts of AM1_1499g1_$F_{97}V/S_{118}C$ and AM1_1499g1_$F_{97}V/S_{118}C/Y_{151}L/T_{159}N$ scarcely showed dark reversion during the observed time range (Fig. 2B, D). We detected an increased absorption around 580 and 560 nm for AM1_1499g1_$S_{118}C$ and AM1_1499g1_$S_{118}C/Y_{151}L/T_{159}N$, respectively (Fig. 2A, C). The dark reversion of AM1_1499g1_$S_{118}C$ (Fig. 2A) was

198 remarkably faster than that of AM1_1499g1_S_{118}C/Y_{151}L/T_{159}N (Fig. 2C). These results
199 support our hypothesis that the twisted states are more likely to show dark reversion.
200 By contrast, both twisted and relaxed photoproduct states of
201 AM1_1499g1_S_{118}C/H_{128}Y and F_{97}V/S_{118}C/H_{128}Y showed no detectable dark reversion
202 during the observed time range. These results suggest a difference in stability of photoproduct
203 states between the DXCF CBCRs with and without second Cys ligation activity, although the
204 second Cys ligation occurs in the dark state instead of the photoproduct state. Although the
205 absorbance around 415 nm of both molecules slightly increased with time, we could not
206 detect clear isosbestic points around 360 nm (Fig. 2E, F). Therefore, this slight increase of
207 absorbance was not due to the dark reversion but rather due to the light scattering caused by
208 protein aggregation under relatively high temperature of 30°C.
209
210 **Dark stability of the photoproduct states of the molecules lacking ligation activity of**
211 **second Cys**
212 To further investigate the relationship between the ring D geometry and the dark reversion
213 kinetics, we focused on green/teal-reversible AM1_6305g1, a close homolog of
214 AM1_1499g1, which lacks the ligation activity of the second Cys and forms a subfamily with
215 blue/teal reversible (NpR1597g1[18] and NpR5113g1[18]) and green/teal reversible (FdDpxAg[24])
216 CBCRs (Fig. S2B). In the previous study, we have constructed a variant molecule,
217 AM1_6305g1_L_{132}Y/N_{140}T, which showed yellow/teal reversible photoconversion.[38] The
218 teal-absorbing photoproduct states of these two molecules appeared to be the twisted type.
219 Thus, we introduced F_{78}V replacement in these two molecules to cancel the trapped geometry
220 of ring D, generating the relaxed type of variants, AM1_6305g1_F_{78}V and
221 AM1_6305g1_F_{78}V/L_{132}Y/N_{140}T (Fig. S2C–E). Consequently, the photoproduct states of
222 these two molecules are about 20–30 nm red shifted in absorbing green light in comparison

with those of the parent molecules (Fig. S2D, E),[7,38] confirming that these photoproduct states adopt the relaxed ring D geometry.

We next examined the dark stability of the photoproduct states of these four molecules under the same condition as the experiments for AM1_1499g1 variants (i.e. monitoring for 5 hours at 30ºC) (Fig. 3A–D). As expected, the twisted photoproduct states of the wild-type and AM1_6305g1_$L_{132}Y/N_{140}T$ showed dark reversion, whereas the relaxed states of AM1_6305g1_$F_{78}V$ and AM1_6305g1_$F_{78}V/L_{132}Y/N_{140}T$ scarcely showed dark reversion (Fig. 3A–D and Table 1). This observation is notably consistent with that from AM1_1499g1, supporting our hypothesis that the twisted ring D is less thermodynamically stable than the relaxed one.

Dark reversion kinetics

Dark reversion half-life of the variant molecules was calculated from the slope of absorbance increase during each transition process in the logarithmic plots to quantitatively estimate the dark reversion kinetics of the variant proteins showing the detectable dark reversion (Fig. 4 and Table 1). Half-life for AM1_1499g1_$S_{118}C$ and $S_{118}C/Y_{151}L/T_{159}N$ (twisted type) was 5.99 h ± 0.31 and 22.6 h ± 1.31, respectively, whereas that for $F_{97}V/S_{118}C$ and $F_{97}V/S_{118}C/Y_{151}L/T_{159}N$ (relaxed type) was 52.6 h ± 3.05 and 53.1 h ± 35.8, respectively (Fig. 4A, B and Table 1). Moreover, the half-life for AM1_6305g1 and $L_{132}Y/N_{140}T$ (twisted type) was 31.8 h ± 4.59 and 131.0 h ± 24.6, respectively, whereas that for $F_{78}V$ and $F_{78}V/L_{132}Y/N_{140}T$ (relaxed type) was 85.5 h ± 11.5 and 262.1 h ± 85.7, respectively (Fig. 4C, D and Table 1). Statistical analyses showed that the kinetics of the DXCF CBCRs incorporating the “twisted” chromophore were significantly more rapid than that of the DXCF CBCRs incorporating the “relaxed” one (Fig. 4 and Table 1).

Dark stability of the photoproduct states of the molecules with reversible Cys adduct formation irrespective of ring D configuration

We found that neither AM1_1499g1_$S_{118}C/H_{128}Y$ nor $F_{97}V/S_{118}C/H_{128}Y$ showed detectable dark reversion during the observed time range (Fig. 2E, F), suggesting that second Cys-adducting capability contributes to the photoproduct stability, whether the photoproduct ring D is twisted or relaxed. To test this hypothesis, we focused on NpR5113g3, which forms a subfamily with AM1_1499g1 and AM1_6305g1 (Fig. S2B) but showed reversible Cys adduct formation with blue/teal photocycle (Fig. S3).[18] As expected, similar to AM1_1499g1_$S_{118}C/H_{128}Y$, the twisted photoproduct state of NpR5113g3 did not show detectable dark reversion (Fig. 2E and S3).

To test our hypothesis on molecules outside of this subfamily, we focused on another CBCR, AM1_0048g1. AM1_0048g1 belongs to a subfamily distinct from the AM1_1499g1 subfamily (Fig. S2B) while retaining the DXCF Cys residue that shows reversible Cys adduct formation with blue/teal photocycle similar to NpR5113g3. We monitored its dark reversion process from the teal-absorbing photoproduct state to the blue-absorbing dark state (Fig. 3E).[7] We found that the twisted photoproduct state of AM1_0048g1 did not show detectable dark reversion, similar to AM1_1499g1_$S_{118}C/H_{128}Y$ and NpR5113g3 (Figs. 2E, 3E, and S3 and Table 1). Moreover, we constructed a variant protein, AM1_0048g1_$F_{241}V/F_{298}L$, to cancel the twisted ring D geometry of the photoproduct state. The photoproduct state of AM1_0048g1_$F_{241}V/F_{298}L$ is 8 nm red shifted in comparison with that of the wild-type protein (Fig. S2C, F).[7] As expected, the relaxed photoproduct state of this variant did not show detectable dark reversion (Fig. 3F and Table 1).

Discussion

In this study, we investigated the relationship between the photoproduct ring D geometry (twisted or relaxed) of the PVB chromophore and the dark reversion kinetics of the DXCF CBCRs. In the DXCF CBCRs without reversible Cys adduct formation, the twisted photoproduct states, but not the relaxed photoproduct states, showed dark reversion to the dark states (Figs. 2A–D and 3A–D). These results strongly support our hypothesis that twisted geometry of the rotating ring D results in instability of the photoproduct state, promoting dark reversion. By contrast, in the DXCF CBCRs with reversible Cys adduct formation, neither twisted nor relaxed state showed detectable dark reversion (Figs. 2E, F, 3E, F, and S3). These results indicate that reversible ligation activity of the second Cys in the dark state affects the photoproduct stability, although the photoproduct state does not form a covalent bond with the second Cys. Therefore, positioning of the second Cys residue in the photoproduct state may vary between the molecules with and without reversible Cys adducting capability. In fact, it has been reported that the second Cys of TePixJg, a typical DXCF CBCR with reversible Cys-adduct formation, showed large conformational change upon photoconversion.[26,28] Particularly, the side chain of the free second Cys in the photoproduct state faces a direction opposite from the chromophore (Fig. S1A, B). This movement would result in structural changes of the conserved Asp residue in the DXCF motif that interacts with the ring D nitrogen. Such dynamic rearrangement of the second Cys and Asp residues may also occur in the molecules analyzed here, which may contribute to stabilization of the twisted ring D in the photoproduct state. Structural studies are needed to address the detailed molecular mechanisms underlying these phenomena.

We have previously found that atypical DXCF CBCRs with unique sequence arrangement showed dark reversion; cce_4193g1 retains the second Cys but not the first Cys[5]; AM1_1870g4 has an arranged DXCF motif, in which the Asp residue is swapped with

296 the next residue.[7] Our previous study suggested that the chemical environment near the
297 DXCF motif affects the 15*E*–chromophore stability, consistent with the observation in this
298 study.

299 It has been reported that some molecules belonging to the extended red/green (XRG)
300 CBCR subfamily show dark reversion from the green-absorbing photoproduct state to the
301 red-absorbing dark state, whereas others do not.[6,20,44] Previous structural and spectral studies
302 elucidated that the photoproduct state of the XRG CBCRs adopted highly twisted ring D,
303 which absorbs shorter-wavelength green light despite PCB incorporation (Fig. S1C).[29,35] This
304 twisted ring D is fixed by the two Phe residues on the α–helix and the β–sheet conserved in
305 many XRG CBCRs (Fig. S1C and S2B). Replacement of these Phe residues with non-
306 aromatic ones, such as Val and Leu, results in red shift of the photoproduct absorption
307 compared with their parent molecules.[39,45] Although dark reversion kinetics of these variant
308 molecules remains unclear, a trend similar to that observed in this study should be expected.

309 On the other hand, some atypical XRG CBCRs categorized into insert Cys subfamily
310 have another second Cys residue within an inserted loop structure, which has a reversible
311 ligation activity as well as the second Cys of the DXCF CBCRs.[17,23,33,46] Cho et al. have
312 reported that Mbr3854g4 (UG1) and Mbl3738g2 (UG2) of the insert Cys CBCRs did not
313 show detectable dark reversion.[46] UG1 and UG2 possess aromatic amino acids on the α–helix
314 and the β–sheet, whose replacement resulted in red-shift of the photoproduct, indicating that
315 trapped-twist model is also applicable to this subfamily.[46] In summary, the twisted insert Cys
316 CBCRs with the reversible Cys ligation activity did not show dark reversion, which is
317 comparable to the twisted DXCF CBCRs with the reversible Cys ligation activity. Lack of
318 the ligation activity is again suggested to be the driving force of the photoproduct instability.

319 To date, color tuning by replacing specific Phe residue(s) has been done in the DXCF
320 CBCRs in the AM1_1499g1 subfamily and some XRG CBCRs.[38,39,45] The photoproduct

states of these variant molecules are red shifted in comparison with those of their parent molecules due to cancellation of the ring D twist. In this study, we successfully canceled the trapped-twist of the photoproduct state of two different DXCF CBCR scaffolds, AM1_6305g1 and AM1_0048g1 (Fig. S2C–E). As AM1_0048g1 belongs to a subfamily distinct from the AM1_1499g1 subfamily (Fig. S2B), our results provide a new approach to modify sensing light quality of a wide variety of CBCRs, which will improve fine tuning of the optogenetic and fluorescent templates.[6,20,27,38,44,47–49]

Conflicts of interest

There are no conflicts to declare.

Acknowledgments

This work was supported by grants from JST, CREST (JPMJCR1653 to R.N.). The authors would like to thank Enago (www.enago.jp) for the English language review.

References

1 A. N. Bussell and D. M. Kehoe, Control of a four-color sensing photoreceptor by a two-color sensing photoreceptor reveals complex light regulation in cyanobacteria, *Proc. Natl. Acad. Sci. U. S. A.*, 2013, **110**, 12834–12839.

2 Y. Chen, J. Zhang, J. Luo, J.-M. Tu, X.-L. Zeng, J. Xie, M. Zhou, J.-Q. Zhao, H. Scheer and K.-H. Zhao, Photophysical diversity of two novel cyanobacteriochromes with phycocyanobilin chromophores: photochemistry and dark reversion kinetics, *FEBS J.*, 2012, **279**, 40–54.

3 G. Enomoto, Y. Hirose, R. Narikawa and M. Ikeuchi, Thiol-based photocycle of the blue and teal light-sensing cyanobacteriochrome Tlr1999, *Biochemistry*, 2012, **51**, 3050–3058.

4 K. Fushimi, T. Nakajima, Y. Aono, T. Yamamoto, Ni-Ni-Win, M. Ikeuchi, M. Sato and R. Narikawa, Photoconversion and fluorescence properties of a red/green-type cyanobacteriochrome AM1_C0023g2 that binds not only phycocyanobilin but also biliverdin, *Front. Microbiol.*, 2016, **7**, 588.

5 K. Fushimi, N. C. Rockwell, G. Enomoto, Ni-Ni-Win, S. S. Martin, F. Gan, D. A. Bryant, M. Ikeuchi, J. C. Lagarias and R. Narikawa, Cyanobacteriochrome photoreceptors lacking the canonical Cys residue, *Biochemistry*, 2016, **55**, 6981–6995.

6 K. Fushimi, G. Enomoto, M. Ikeuchi and R. Narikawa, Distinctive properties of dark reversion kinetics between two red/green-type cyanobacteriochromes and their application in the photoregulation of cAMP synthesis, *Photochem. Photobiol.*, 2017, **93**, 681–691.

7 M. Hasegawa, K. Fushimi, K. Miyake, T. Nakajima, Y. Oikawa, G. Enomoto, M. Sato, M. Ikeuchi and R. Narikawa, Molecular characterization of DXCF cyanobacteriochromes from the cyanobacterium *Acaryochloris marina* identifies a blue-

light power sensor, *J. Biol. Chem.*, 2018, **293**, 1713–1727.

8 Y. Hirose, T. Shimada, R. Narikawa, M. Katayama and M. Ikeuchi, Cyanobacteriochrome CcaS is the green light receptor that induces the expression of phycobilisome linker protein, *Proc. Natl. Acad. Sci. U. S. A.*, 2008, **105**, 9528–9533.

9 Y. Hirose, R. Narikawa, M. Katayama and M. Ikeuchi, Cyanobacteriochrome CcaS regulates phycoerythrin accumulation in *Nostoc punctiforme*, a group II chromatic adapter, *Proc. Natl. Acad. Sci. U. S. A.*, 2010, **107**, 8854–8859.

10 Y. Hirose, N. C. Rockwell, K. Nishiyama, R. Narikawa, Y. Ukaji, K. Inomata, J. C. Lagarias and M. Ikeuchi, Green/red cyanobacteriochromes regulate complementary chromatic acclimation via a protochromic photocycle, *Proc. Natl. Acad. Sci. U. S. A.*, 2013, **110**, 4974–4979.

11 T. Ishizuka, T. Shimada, K. Okajima, S. Yoshihara, Y. Ochiai, M. Katayama and M. Ikeuchi, Characterization of cyanobacteriochrome TePixJ from a thermophilic cyanobacterium *Thermosynechococcus elongatus* strain BP-1, *Plant Cell Physiol.*, 2006, **47**, 1251–1261.

12 Q. Ma, H.-H. Hua, Y. Chen, B.-B. Liu, A. L. Krämer, H. Scheer, K.-H. Zhao and M. Zhou, A rising tide of blue-absorbing biliprotein photoreceptors: Characterization of seven such bilin-binding GAF domains in *Nostoc* sp. PCC 7120, *FEBS J.*, 2012, **279**, 4095–4108.

13 R. Narikawa, Y. Fukushima, T. Ishizuka, S. Itoh and M. Ikeuchi, A novel photoactive GAF domain of cyanobacteriochrome AnPixJ that shows reversible green/red photoconversion, *J. Mol. Biol.*, 2008, **380**, 844–855.

14 R. Narikawa, T. Kohchi and M. Ikeuchi, Characterization of the photoactive GAF domain of the CikA homolog (SyCikA, Slr1969) of the cyanobacterium *Synechocystis* sp. PCC 6803, *Photochem. Photobiol. Sci.*, 2008, **7**, 1253–1259.

15 R. Narikawa, G. Enomoto, Ni-Ni-Win, K. Fushimi and M. Ikeuchi, A new type of dual-Cys cyanobacteriochrome GAF domain found in cyanobacterium *Acaryochloris marina*, which has an unusual red/blue reversible photoconversion cycle, *Biochemistry*, 2014, **53**, 5051–5059.

16 R. Narikawa, T. Nakajima, Y. Aono, K. Fushimi, G. Enomoto, Ni-Ni-Win, S. Itoh, M. Sato and M. Ikeuchi, A biliverdin-binding cyanobacteriochrome from the chlorophyll *d*–bearing cyanobacterium *Acaryochloris marina*, *Sci. Rep.*, 2015, **5**, 7950.

17 N. C. Rockwell, S. S. Martin, K. Feoktistova and J. C. Lagarias, Diverse two-cysteine photocycles in phytochromes and cyanobacteriochromes, *Proc. Natl. Acad. Sci. U. S. A.*, 2011, **108**, 11854–11859.

18 N. C. Rockwell, S. S. Martin, A. G. Gulevich and J. C. Lagarias, Phycoviolobilin formation and spectral tuning in the DXCF cyanobacteriochrome subfamily, *Biochemistry*, 2012, **51**, 1449–1463.

19 N. C. Rockwell, S. S. Martin and J. C. Lagarias, Mechanistic insight into the photosensory versatility of DXCF cyanobacteriochromes, *Biochemistry*, 2012, **51**, 3576–3585.

20 N. C. Rockwell, S. S. Martin and J. C. Lagarias, Red/green cyanobacteriochromes: sensors of color and power, *Biochemistry*, 2012, **51**, 9667–9677.

21 N. C. Rockwell, S. S. Martin and J. C. Lagarias, Identification of DXCF cyanobacteriochrome lineages with predictable photocycles, *Photochem. Photobiol. Sci.*, 2015, **14**, 929–941.

22 N. C. Rockwell, S. S. Martin and J. C. Lagarias, Identification of cyanobacteriochromes detecting far-red Light, *Biochemistry*, 2016, **55**, 3907–3919.

23 N. C. Rockwell, S. S. Martin and J. C. Lagarias, There and back again: Loss and reacquisition of two-Cys photocycles in cyanobacteriochromes, *Photochem. Photobiol.*,

2017, **93**, 741–754.

24 L. B. Wiltbank and D. M. Kehoe, Two cyanobacterial photoreceptors regulate photosynthetic light harvesting by sensing teal, green, yellow, and red light, *MBio*, 2016, **7**, e02130–15.

25 S. Yoshihara, M. Katayama, X. Geng and M. Ikeuchi, Cyanobacterial phytochrome-like PixJ1 holoprotein shows novel reversible photoconversion between blue- and green-absorbing forms, *Plant Cell Physiol.*, 2004, **45**, 1729–1737.

26 E. S. Burgie, E. Sethe Burgie, J. M. Walker, G. N. Phillips and R. D. Vierstra, Crystal structure of the photosensing module from a red/far-red light-absorbing plant phytochrome, *Structure*, 2013, **21**, 88–97.

27 K. Fushimi, T. Miyazaki, Y. Kuwasaki, T. Nakajima, T. Yamamoto, K. Suzuki, Y. Ueda, K. Miyake, Y. Takeda, J.-H. Choi, H. Kawagishi, E. Y. Park, M. Ikeuchi, M. Sato and R. Narikawa, Rational conversion of chromophore selectivity of cyanobacteriochromes to accept mammalian intrinsic biliverdin, *Proc. Natl. Acad. Sci. U. S. A.*, 2019, **116**, 8301–8309.

28 R. Narikawa, T. Ishizuka, N. Muraki, T. Shiba, G. Kurisu and M. Ikeuchi, Structures of cyanobacteriochromes from phototaxis regulators AnPixJ and TePixJ reveal general and specific photoconversion mechanism, *Proc. Natl. Acad. Sci. U. S. A.*, 2013, **110**, 918–923.

29 X. Xu, A. Port, C. Wiebeler, K.-H. Zhao, I. Schapiro and W. Gärtner, Structural elements regulating the photochromicity in a cyanobacteriochrome, *Proc. Natl. Acad. Sci. U. S. A.*, 2020, **117**, 2432–2440.

30 K. Anders, G. Daminelli-Widany, M. A. Mroginski, D. von Stetten and L.-O. Essen, Structure of the cyanobacterial phytochrome 2 photosensor implies a tryptophan switch for phytochrome signaling, *J. Biol. Chem.*, 2013, **288**, 35714–35725.

435 31 E. S. Burgie, A. N. Bussell, J. M. Walker, K. Dubiel and R. D. Vierstra, Crystal
436 structure of the photosensing module from a red/far-red light-absorbing plant
437 phytochrome, *Proc. Natl. Acad. Sci. U. S. A.*, 2014, **111**, 10179–10184.
438 32 L.-O. Essen, J. Mailliet and J. Hughes, The structure of a complete phytochrome sensory
439 module in the Pr ground state, *Proc. Natl. Acad. Sci. U. S. A.*, 2008, **105**, 14709–14714.
440 33 K. Fushimi, M. Ikeuchi and R. Narikawa, The expanded red/green cyanobacteriochrome
441 lineage: An evolutionary hot spot, *Photochem. Photobiol.*, 2017, **93**, 903–906.
442 34 K. Fushimi and R. Narikawa, Cyanobacteriochromes: photoreceptors covering the entire
443 UV-to-visible spectrum, *Curr. Opin. Struct. Biol.*, 2019, **57**, 39–46.
444 35 S. Lim, Q. Yu, S. M. Gottlieb, C.-W. Chang, N. C. Rockwell, S. S. Martin, D. Madsen, J.
445 C. Lagarias, D. S. Larsen and J. B. Ames, Correlating structural and photochemical
446 heterogeneity in cyanobacteriochrome NpR6012g4, *Proc. Natl. Acad. Sci. U. S. A.*, 2018,
447 **115**, 4387–4392.
448 36 T. Ishizuka, R. Narikawa, T. Kohchi, M. Katayama and M. Ikeuchi,
449 Cyanobacteriochrome TePixJ of *Thermosynechococcus elongatus* harbors
450 phycoviolobilin as a chromophore, *Plant Cell Physiol.*, 2007, **48**, 1385–1390.
451 37 T. Ishizuka, A. Kamiya, H. Suzuki, R. Narikawa, T. Noguchi, T. Kohchi, K. Inomata
452 and M. Ikeuchi, The cyanobacteriochrome, TePixJ, isomerizes its own chromophore by
453 converting phycocyanobilin to phycoviolobilin, *Biochemistry*, 2011, **50**, 953–961.
454 38 K. Fushimi, M. Hasegawa, T. Ito, N. C. Rockwell, G. Enomoto, Ni-Ni-Win, J. C.
455 Lagarias, M. Ikeuchi and R. Narikawa, Evolution-inspired design of multicolored
456 photoswitches from a single cyanobacteriochrome scaffold, *Proc. Natl. Acad. Sci. U. S.*
457 *A.*, 2020, **117**, 15573–15580.
458 39 N. C. Rockwell, S. S. Martin, A. G. Gulevich and J. C. Lagarias, Conserved
459 phenylalanine residues are required for blue-shifting of cyanobacteriochrome

photoproducts, *Biochemistry*, 2014, **53**, 3118–3130.

40 K. Miyake, K. Fushimi, T. Kashimoto, K. Maeda, Ni-Ni-Win, H. Kimura, M. Sugishima, M. Ikeuchi and R. Narikawa, Functional diversification of two bilin reductases for light perception and harvesting in unique cyanobacterium *Acaryochloris marina* MBIC 11017, *FEBS J.*, DOI:10.1111/febs.15230.

41 K. Mukougawa, H. Kanamoto, T. Kobayashi, A. Yokota and T. Kohchi, Metabolic engineering to produce phytochromes with phytochromobilin, phycocyanobilin, or phycoerythrobilin chromophore in *Escherichia coli*, *FEBS Lett.*, 2006, **580**, 1333–1338.

42 S. Kumar, G. Stecher and K. Tamura, MEGA7: Molecular evolutionary genetics analysis version 7.0 for bigger datasets, *Mol. Biol. Evol.*, 2016, **33**, 1870–1874.

43 E. F. Pettersen, T. D. Goddard, C. C. Huang, G. S. Couch, D. M. Greenblatt, E. C. Meng and T. E. Ferrin, UCSF Chimera-a visualization system for exploratory research and analysis, *J. Comput. Chem.*, 2004, **25**, 1605–1612.

44 X.-J. Wu, H. Yang, Y. Sheng, Y.-L. Zhu and P.-P. Li, Fluorescence properties of a novel cyanobacteriochrome GAF domain from *Spirulina* that exhibits moderate dark reversion, *Int. J. Mol. Sci.*, , DOI:10.3390/ijms19082253.

45 N. C. Rockwell, S. S. Martin, F. Gan, D. A. Bryant and J. C. Lagarias, NpR3784 is the prototype for a distinctive group of red/green cyanobacteriochromes using alternative Phe residues for photoproduct tuning, *Photochem. Photobiol. Sci.*, 2015, **14**, 258–269.

46 S. M. Cho, S. C. Jeoung, J.-Y. Song, J.-J. Song and Y.-I. Park, Hydrophobic residues near the bilin chromophore-binding pocket modulate spectral tuning of insert-Cys subfamily cyanobacteriochromes, *Sci. Rep.*, 2017, **7**, 40576.

47 M. Blain-Hartung, N. C. Rockwell, M. V. Moreno, S. S. Martin, F. Gan, D. A. Bryant and J. C. Lagarias, Cyanobacteriochrome-based photoswitchable adenylyl cyclases (cPACs) for broad spectrum light regulation of cAMP levels in cells, *J. Biol. Chem.*,

2018, **293**, 8473–8483.

48 O. S. Oliinyk, A. A. Shemetov, S. Pletnev, D. M. Shcherbakova and V. V. Verkhusha, Smallest near-infrared fluorescent protein evolved from cyanobacteriochrome as versatile tag for spectral multiplexing, *Nat. Commun.*, 2019, **10**, 279.

49 P. Ramakrishnan and J. J. Tabor, Repurposing *synechocystis* PCC6803 UirS–UirR as a UV-violet/green photoreversible transcriptional regulatory tool in *E. coli*, *ACS Synth. Biol.*, 2016, **5**, 733–740.

Table 1. Photochemical properties of DXCF CBCRs in twisted vs. relaxed states*.

	Photocycle			D-ring	Dark state	Photoproduct state	Kinetics			*t*-test
	Dark	/	Photo	geometry	15*Z*, λ_{max} (nm)	15*E*, λ_{max} (nm)	DR, Half life (h)[#, Δ]			*P* value
AM1_1499g1_S_{118}C	Yellow	/	Teal	Twisted	577	492	6.0	±	0.3	< 0.001
AM1_1499g1_F_{97}V/S_{118}C	Yellow	/	Green	Relaxed	577	515	52.6	±	3.1	
AM1_1499g1_S_{118}C/Y_{151}L/T_{159}N	Green	/	Teal	Twisted	559	492	22.6	±	1.3	< 0.05
AM1_1499g1_F_{97}V/S_{118}C/Y_{151}L/T_{159}N	Green	/	Green	Relaxed	560	524	53.1	±	35.8	
AM1_1499g1_S_{118}C/H_{147}Y	Blue	/	Teal	Twisted	413	492	n.d.			–
AM1_1499g1_F_{97}V/S_{118}C/H_{147}Y	Blue	/	Green	Relaxed	417	513	n.d.			
AM1_6305g1_L_{132}Y/N_{140}T	Yellow	/	Teal	Twisted	576	491	131.0	±	24.6	< 0.05
AM1_6305g1_F_{78}V/L_{132}Y/N_{140}T	Yellow	/	Green	Relaxed	576	513	262.1	±	85.7	
AM1_6305g1	Green	/	Teal	Twisted	558	492	31.8	±	4.6	< 0.005
AM1_6305g1_F_{78}V	Green	/	Green	Relaxed	559	523	85.5	±	11.5	
AM1_0048g1	Blue	/	Teal	Twisted	417	498	n.d.			–
AM1_0048g1_F_{241}V/F_{298}L	Blue	/	Green	Relaxed	421	507	n.d.			

The wild-type molecules of these DXCF CBCRs are categorized into the groups 1 or 2 shown in Fig. S2B.

*These parameters were measured at 30°C.

[#]Half-life of the dark reversion (DR) was calculated from the slope in the logarithmic plots shown in Fig. 4. These values are presented as mean ± standard deviation (n = 3 to 6). Significant difference between the half-lives of DXCF CBCRs of twisted and relaxed types was analyzed by Student's *t*-test.

[Δ]n/d means "not determined."

Figures

Fig. 1. Stereochemistry of phycoviolobilin (PVB). (A–D) Chemical structures of 15*Z*– and 15*E*–PVB incorporated into DXCF CBCRs. "First" (or "canonical") Cys covalently binds to the C3[1] position of the chromophore, whereas "second" (or "DXCF") Cys reversibly attaches to/detaches from C10 position with photoconversion/dark reversion induced by *Z*/*E* isomerization at the C15 position. The attachment of the second Cys residue to 15*Z*–PVB in the dark state (or ground state) (A) and the detachment from 15*E*–PVB of the residue in the photoproduct state (or excited state) (B) are observed in typical DXCF CBCRs. In some atypical DXCF CBCRs, red-shifted absorption caused by the π–conjugated system extended to B-to-D rings in the dark state is observed due to lack of the ligation activity (C). Moreover, some DXCF CBCRs show blue-shifted absorption caused by the π–conjugated system restricted to B-to-C rings in the photoproduct state due to the twisted geometry of the D-ring, called "trapped-twist" mechanism (D). π–conjugated systems are highlighted by corresponding color of their absorption light. (E) Comparison of absorption spectra between the typical and atypical DXCF CBCRs shown in Fig. 1A–D (upper: blue light-absorbing 15*Z*–dark state (^{15Z}Pb) and green light-absorbing 15*E*–photoproduct state (^{15E}Pg); middle: green light-absorbing 15*Z*–dark state (^{15Z}Pg); lower: teal light-absorbing 15*E*–photoproduct state (^{15E}Pt)). (F) Positions of specific Phe residues (green) on an α–helix and a β–sheet (shown in Fig. S2B) of twisted DXCF CBCRs, which contribute to stabilization of a 15*E*–chromophore (light gray). These positions are shown using structural information of TePixJg, a typical DXCF CBCR with 15*E*–PVB incorporated (PDB_ID: 3VV4)[28]. Protein structure is shown by stick and sphere models with the secondary structure shown by the ribbon model.

Fig. 2. Reversible photoconversion and dark reversion of AM1_1499g1 variants. (A, C, E) Dark reversion process of (A) AM1_1499g1_S_{118}C (yellow/teal photocycle), (C) AM1_1499g1_S_{118}C/Y_{151}L/T_{159}N (green/teal photocycle) and (E) AM1_1499g1_S_{118}C/H_{147}Y (blue/teal photocycle) with twisted ring D of 15*E*–PVB (cyan to dark blue). (B, D, F) Dark reversion process of (B) AM1_1499g1_F_{97}V/S_{118}C (yellow/green photocycle), (D) AM1_1499g1_F_{97}V/S_{118}C/Y_{151}L/T_{159}N (green/green photocycle) and (F) AM1_1499g1_F_{97}V/S_{118}C/H_{147}Y (blue/green photocycle) with relaxed ring D of 15*E*–PVB (magenta to dark red). The absorption spectra were measured at 30°C and normalized against each maximum absorption of their dark states (light gray). The transition process from the photoproduct states to the dark states was monitored at 0, 1, 2, 3, 4, and 5 h in dark condition.

Fig. 3. Reversible photoconversion and dark reversion of AM1_1499g1 homologs. (A, C, E) Dark reversion process of (A) AM1_6305g1 (green/teal photocycle), (C) AM1_6305g1_L_{132}Y/N_{140}T (yellow/teal photocycle) and (E) AM1_0048g1 (blue/teal photocycle) with twisted ring D of 15*E*–PVB (cyan to dark blue). (B, D, F) Dark reversion process of (B) AM1_6305g1_F_{78}V (green/green photocycle), (D) AM1_6305g1_F_{78}V/L_{132}Y/N_{140}T (yellow/green photocycle) and (F) AM1_0048g1_F_{241}V/F_{298}L (blue/green photocycle) with relaxed ring D of 15*E*–PVB (magenta to dark red). The absorption spectra and transition process were observed under the same conditions shown in Fig. 2 and normalized against each maximum absorption of their dark states (light gray).

Fig. 4. Dark reversion kinetics of DXCF CBCRs in twisted/relaxed types. The logarithm of normalized difference absorbance ($\Delta A(t)/\Delta A(0)$; $\Delta A(t)$ = transition process – 15*Z*–dark state, $\Delta A(0)$ = 15*E*–photoproduct state – 15*Z*–dark state), at each time point (h) was plotted as mean ± standard deviation (n = 3 to 6). DXCF CBCRs in twisted type (cyan) and relaxed type (magenta), and significant difference between them analyzed by the Student's *t*-test (**P* < 0.05, ***P* < 0.005, and ****P* < 0.001, respectively) are shown in each plot. (A) AM1_1499g1_S_{118}C and F_{97}V/S_{118}C; (B) AM1_1499g1_S_{118}C/Y_{151}L/T_{159}N and F_{97}V/S_{118}C/Y_{151}L/T_{159}N; (C) AM1_6305g1 and F_{78}V; (D) AM1_6305g1_L_{132}Y/N_{140}T and F_{78}V/L_{132}Y/N_{140}T. Half-life was calculated from the slope of each plot. The absorbance of the proteins was measured at the wavelength of each maximum absorption of the dark states (peak area of their absorption spectra shown in Figs. 2 and 3).

A

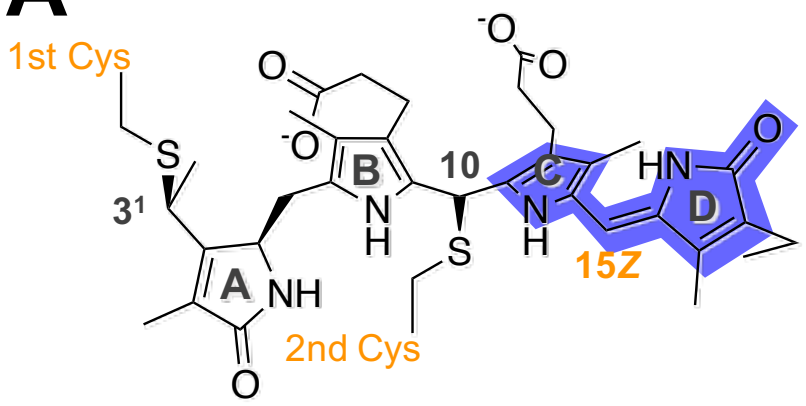

Attached form

B

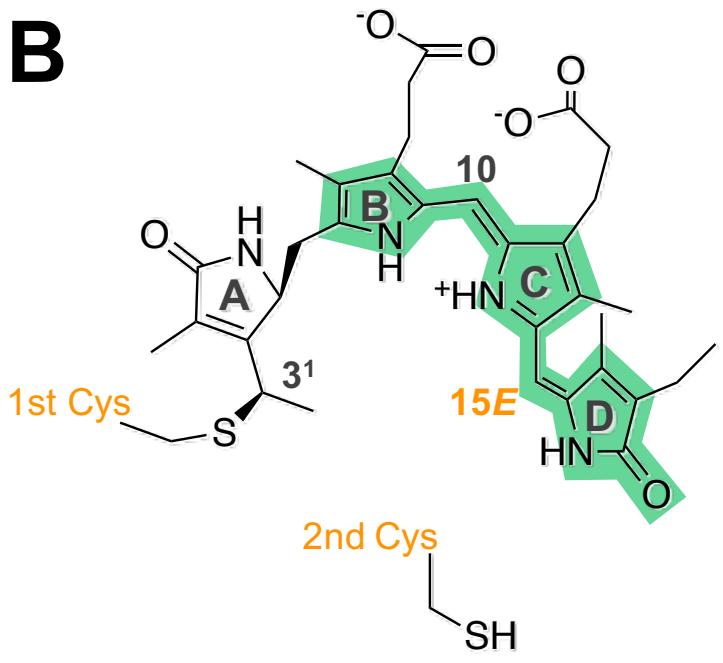

Relaxed form

C

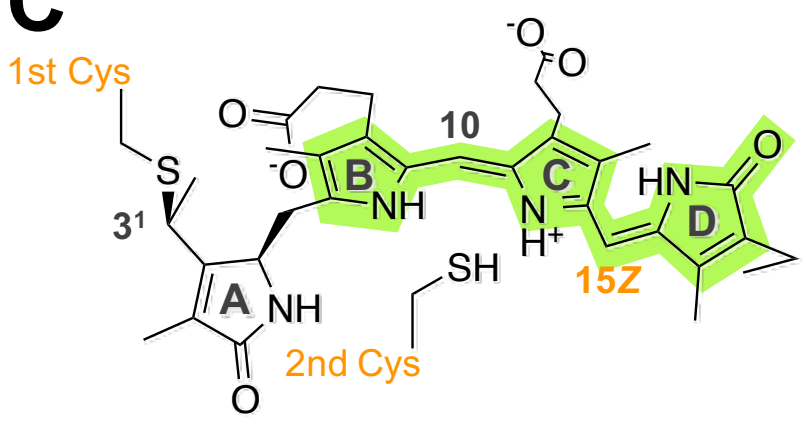

Detached form

D

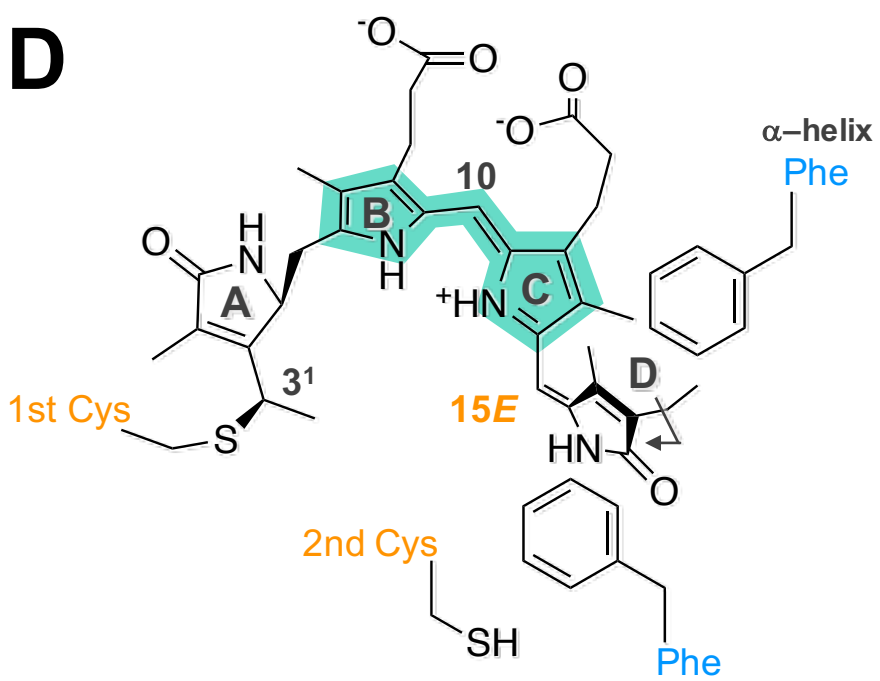

Twisted form

E

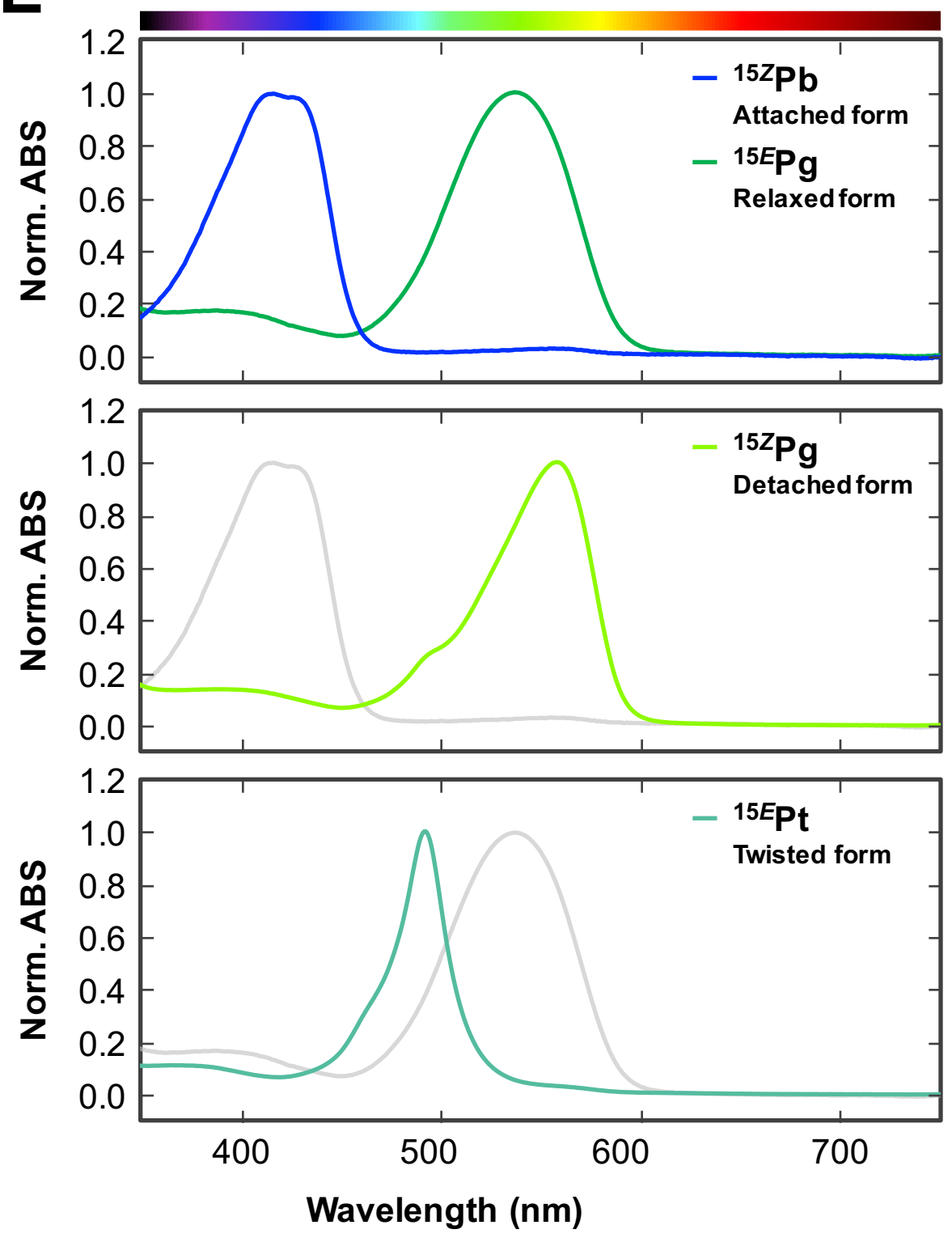

F

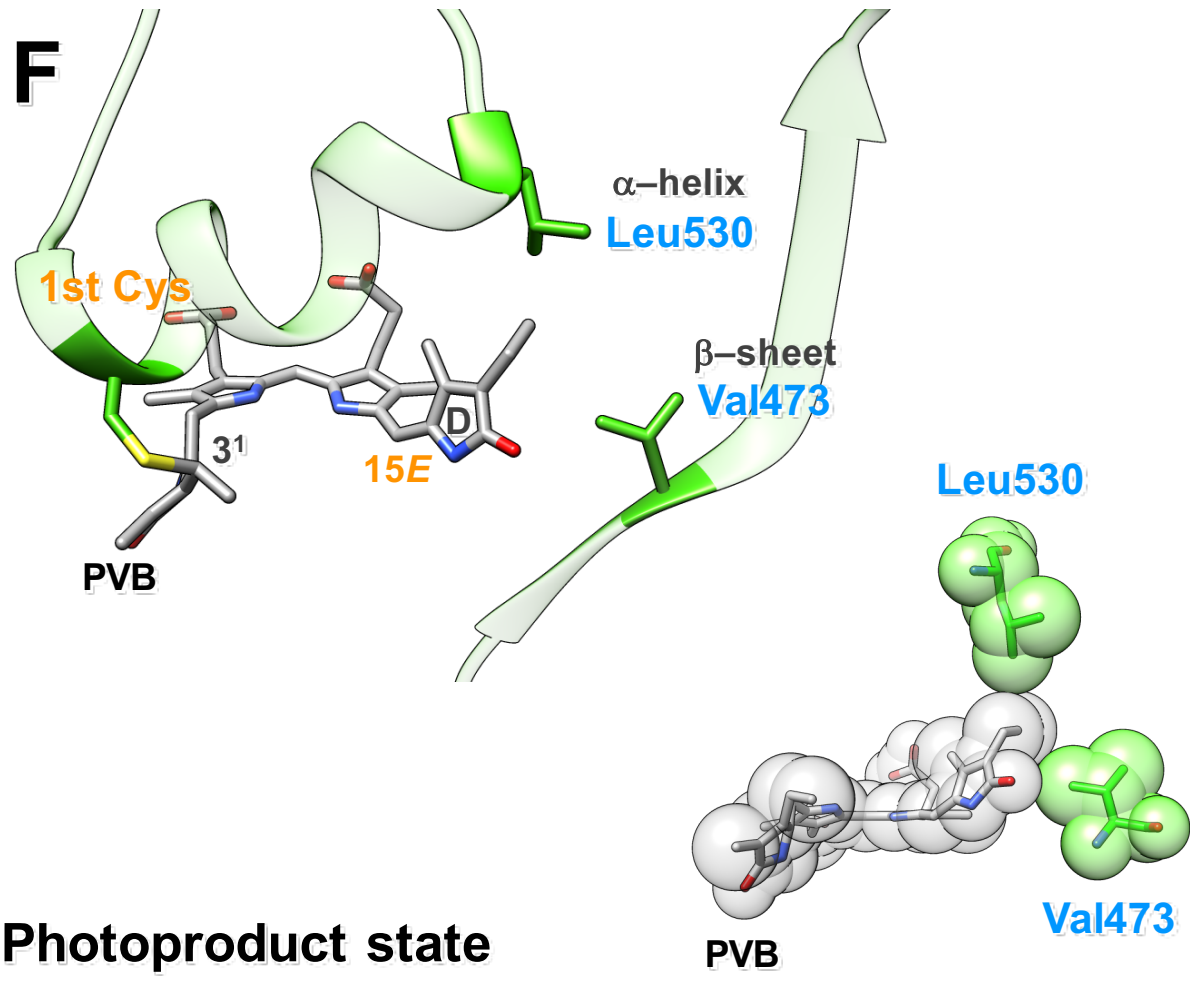

Photoproduct state

A

AM1_1499g1_$S_{118}C$

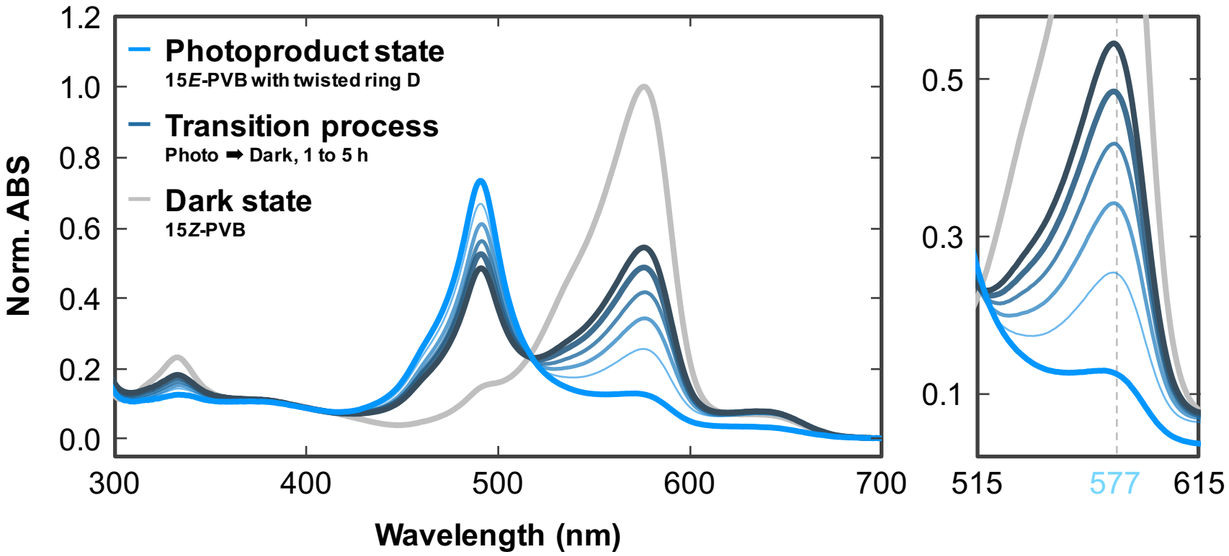

B

AM1_1499g1_$F_{97}V/S_{118}C$

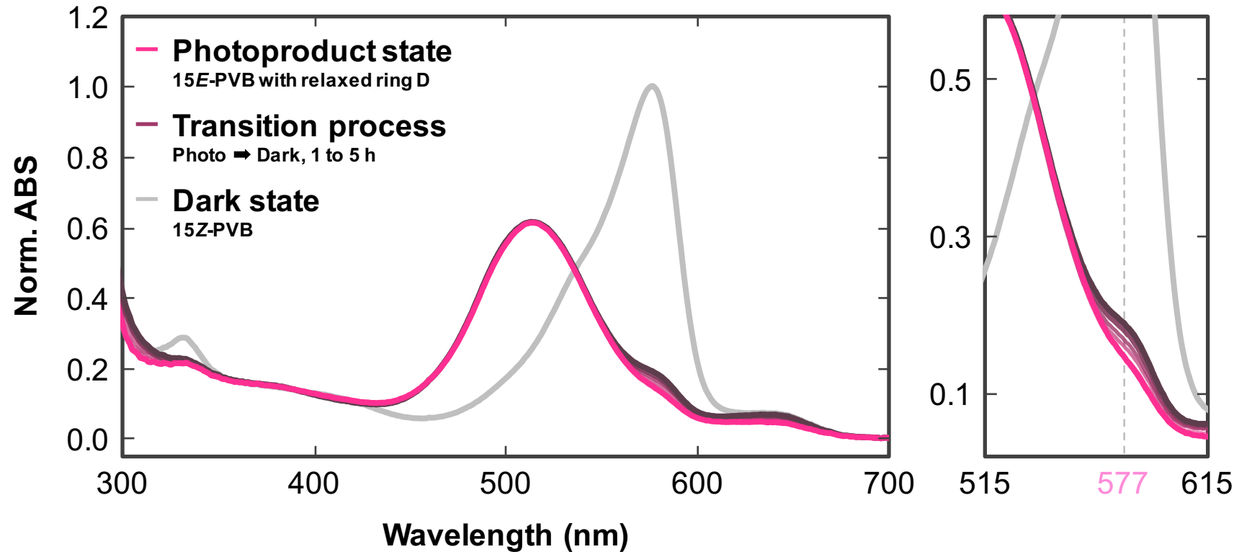

C

AM1_1499g1_$S_{118}C/Y_{151}L/T_{159}N$

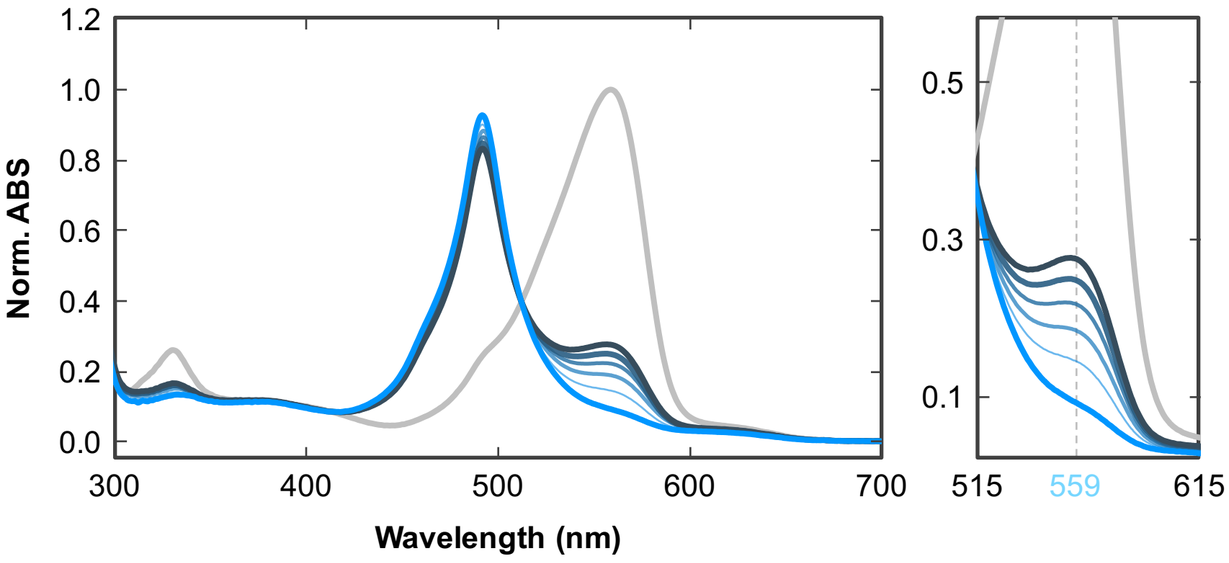

D

AM1_1499g1_$F_{97}V/S_{118}C/Y_{151}L/T_{159}N$

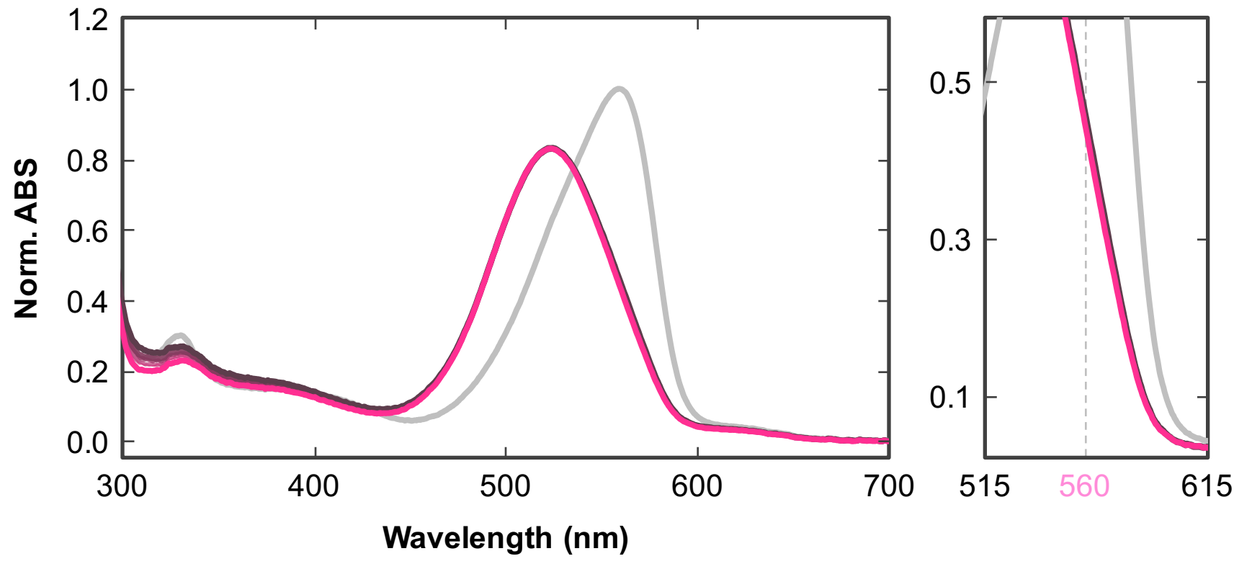

E

AM1_1499g1_$S_{118}C/H_{147}Y$

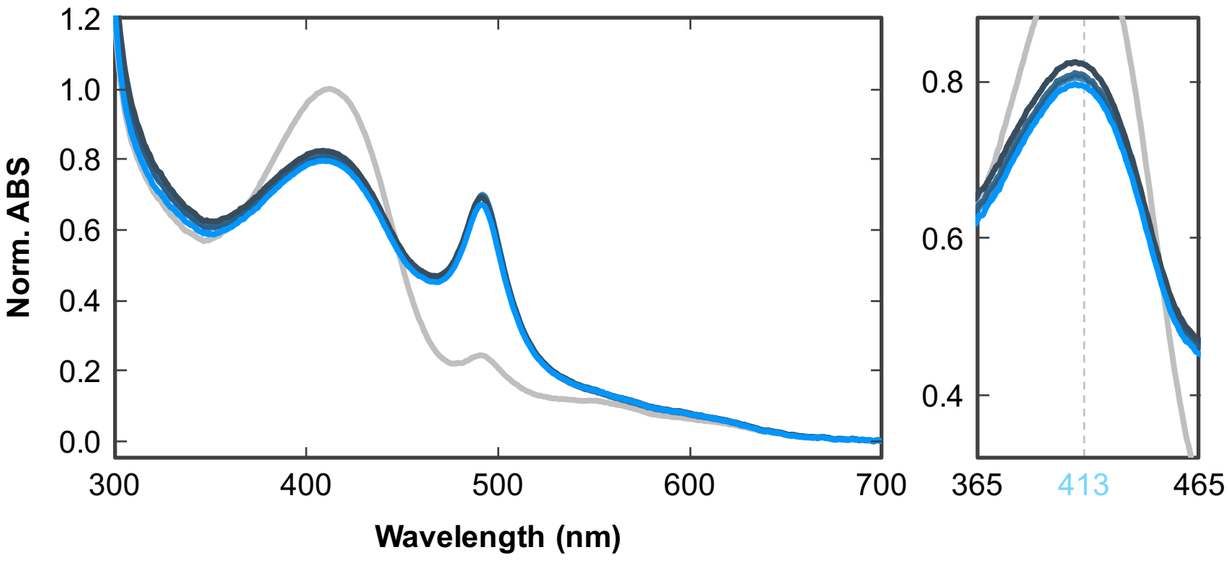

F

AM1_1499g1_$F_{97}V/S_{118}C/H_{147}Y$

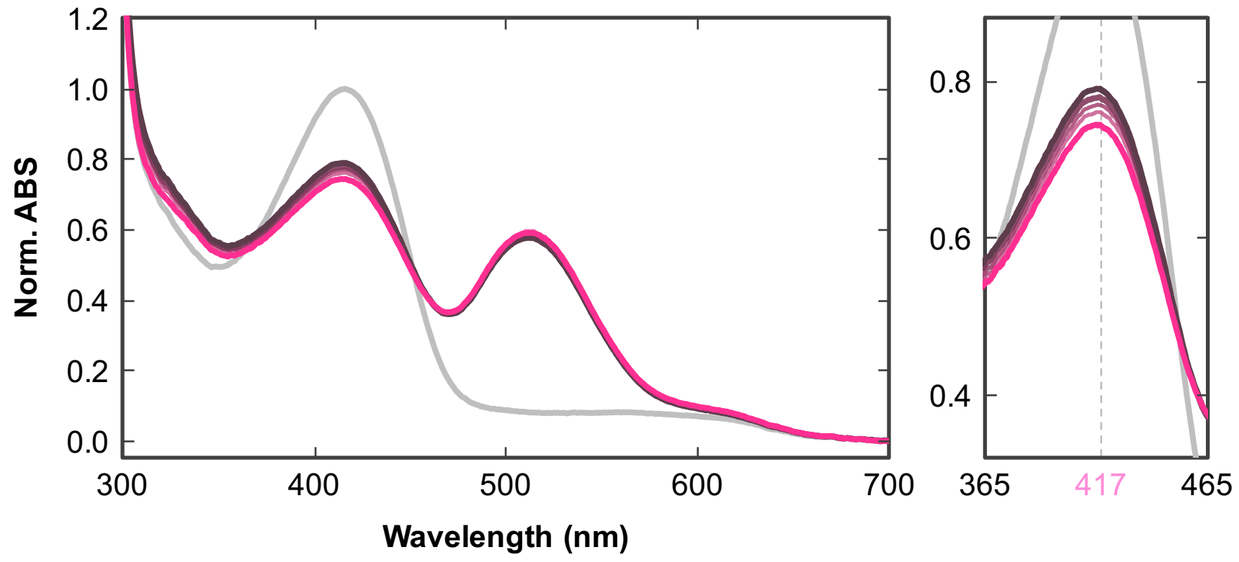

A

AM1_6305g1

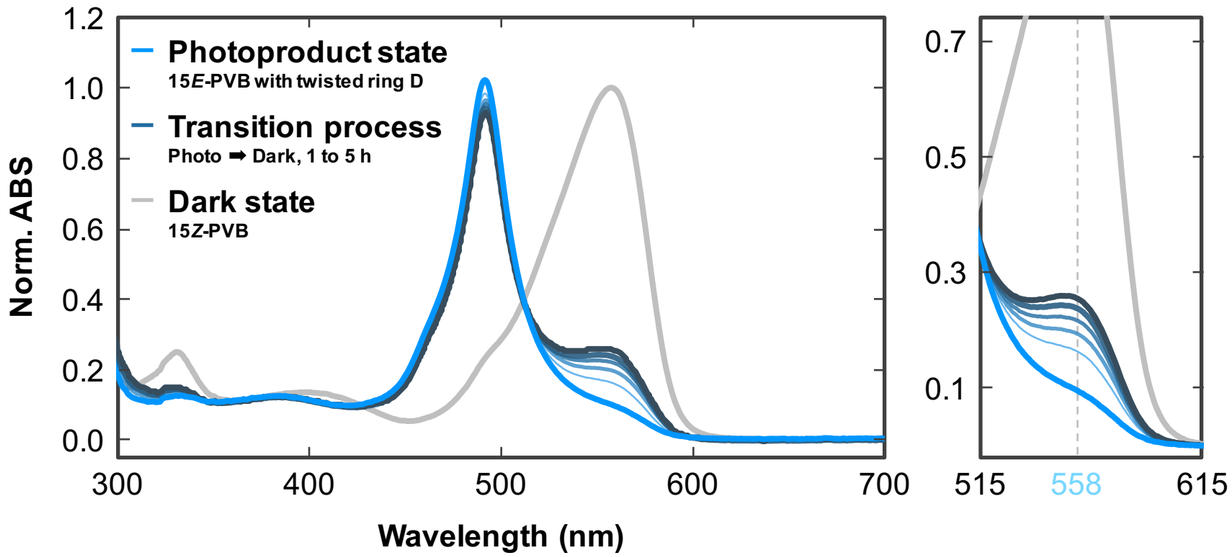

B

AM1_6305g1_$F_{78}V$

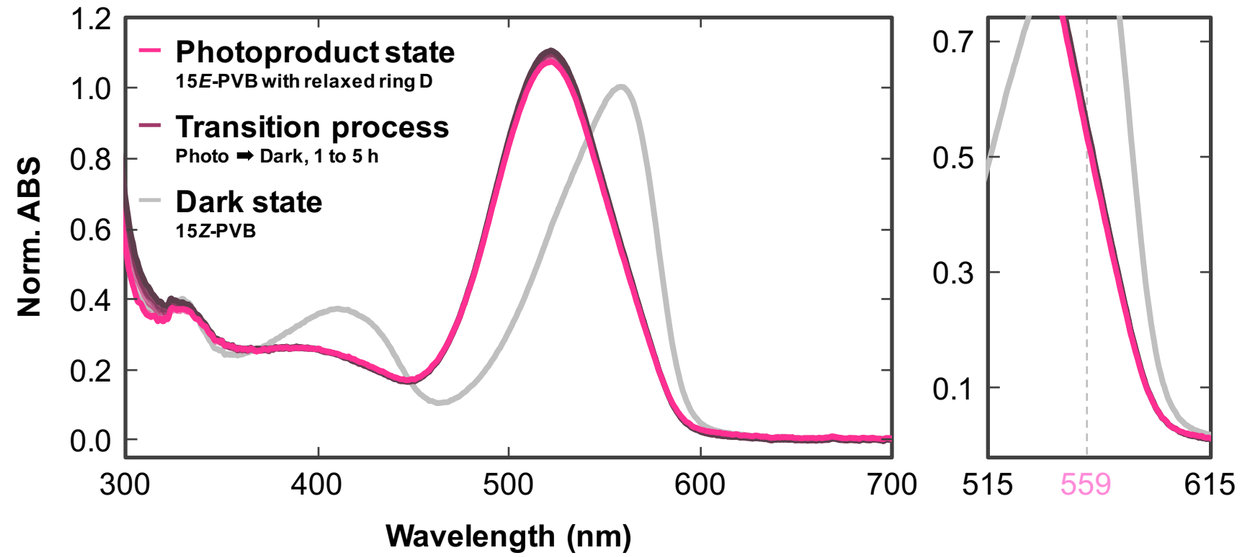

C

AM1_6305g1_$L_{132}Y/N_{140}T$

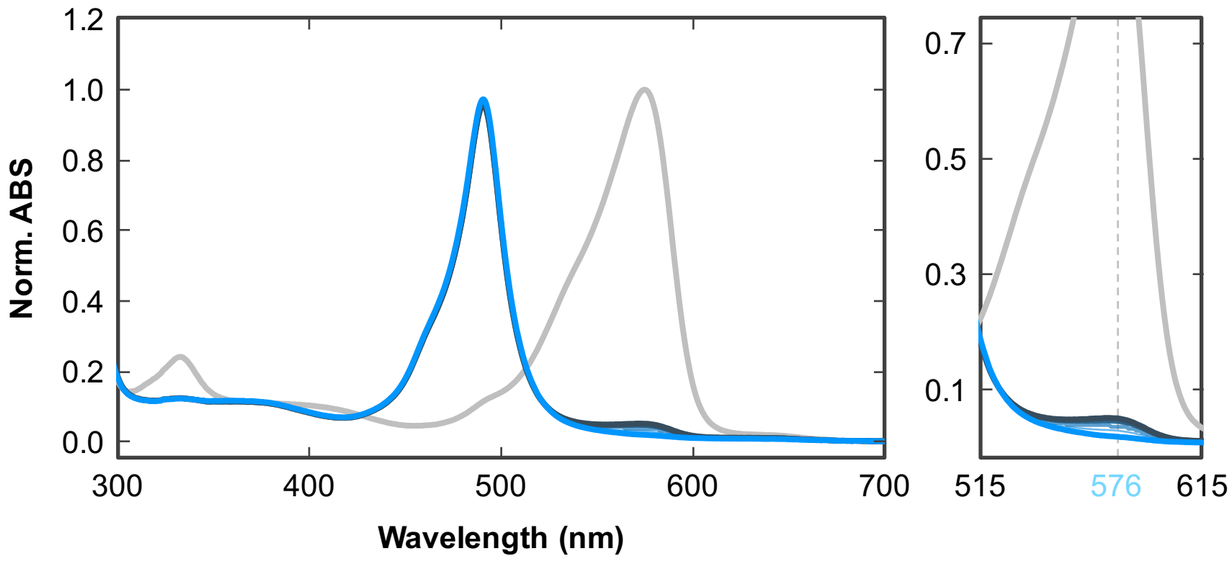

D

AM1_6305g1_$F_{78}V/L_{132}Y/N_{140}T$

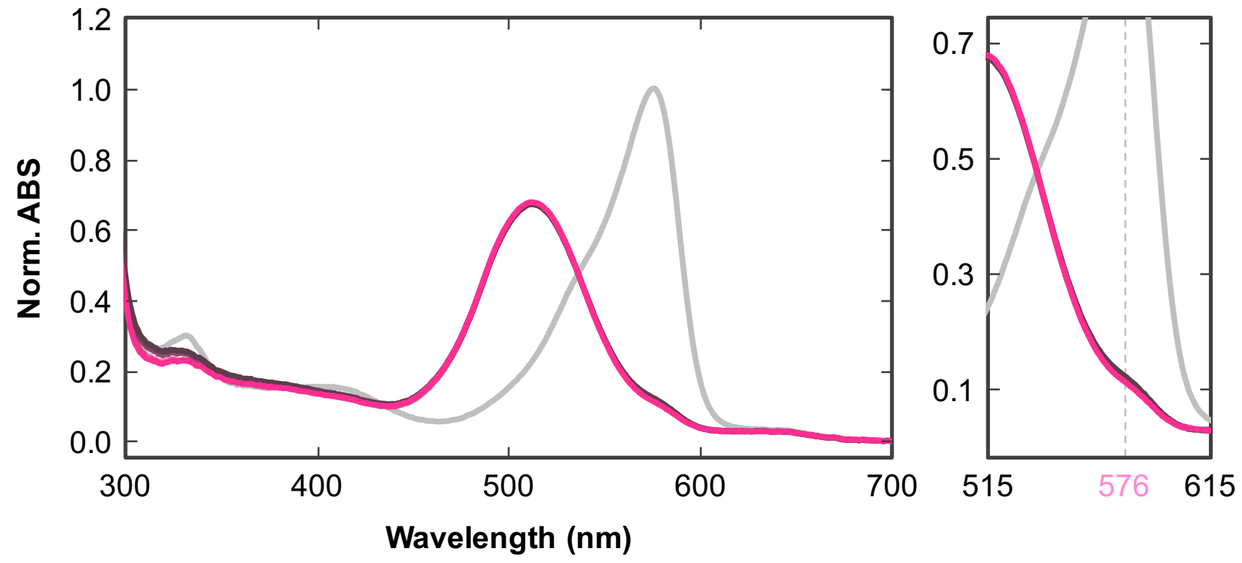

E

AM1_0048g1

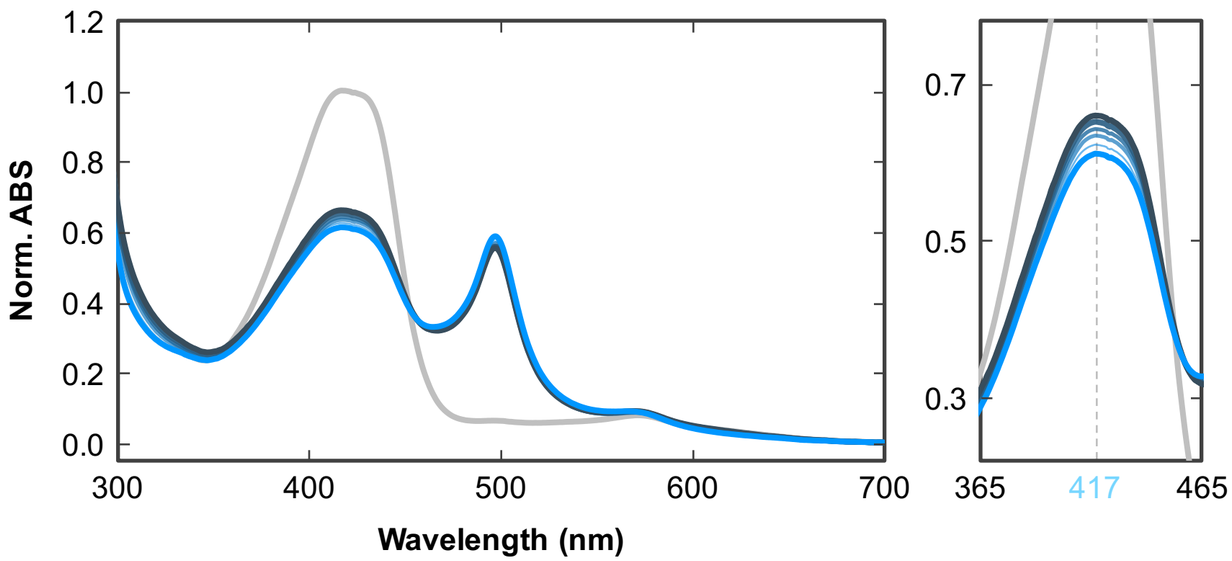

F

AM1_0048g1_$F_{241}V/F_{298}L$

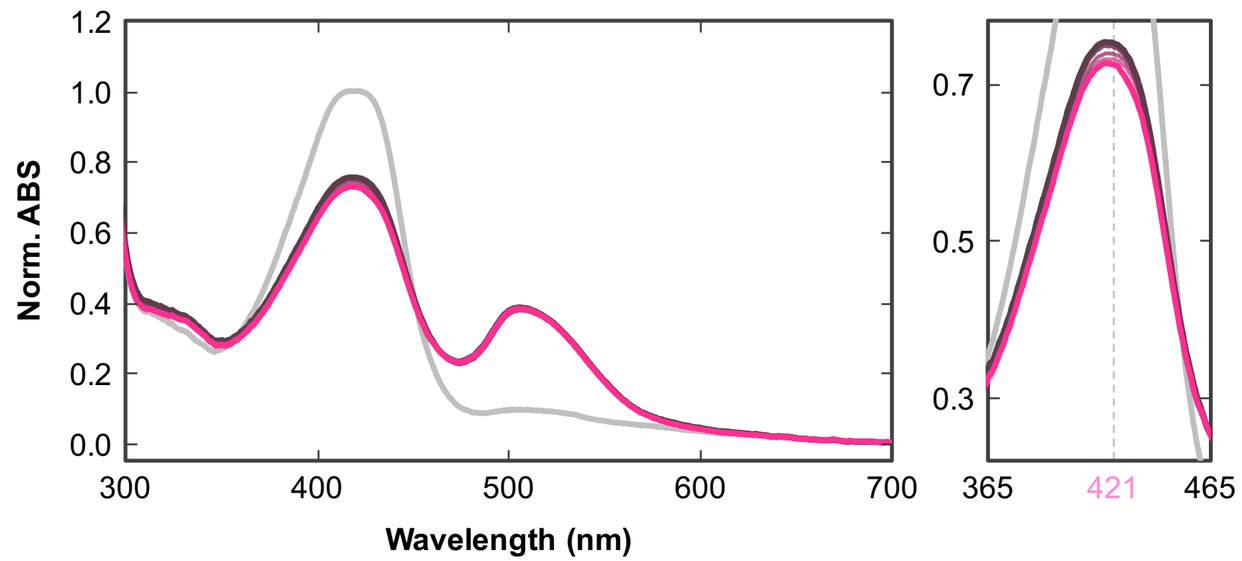

A

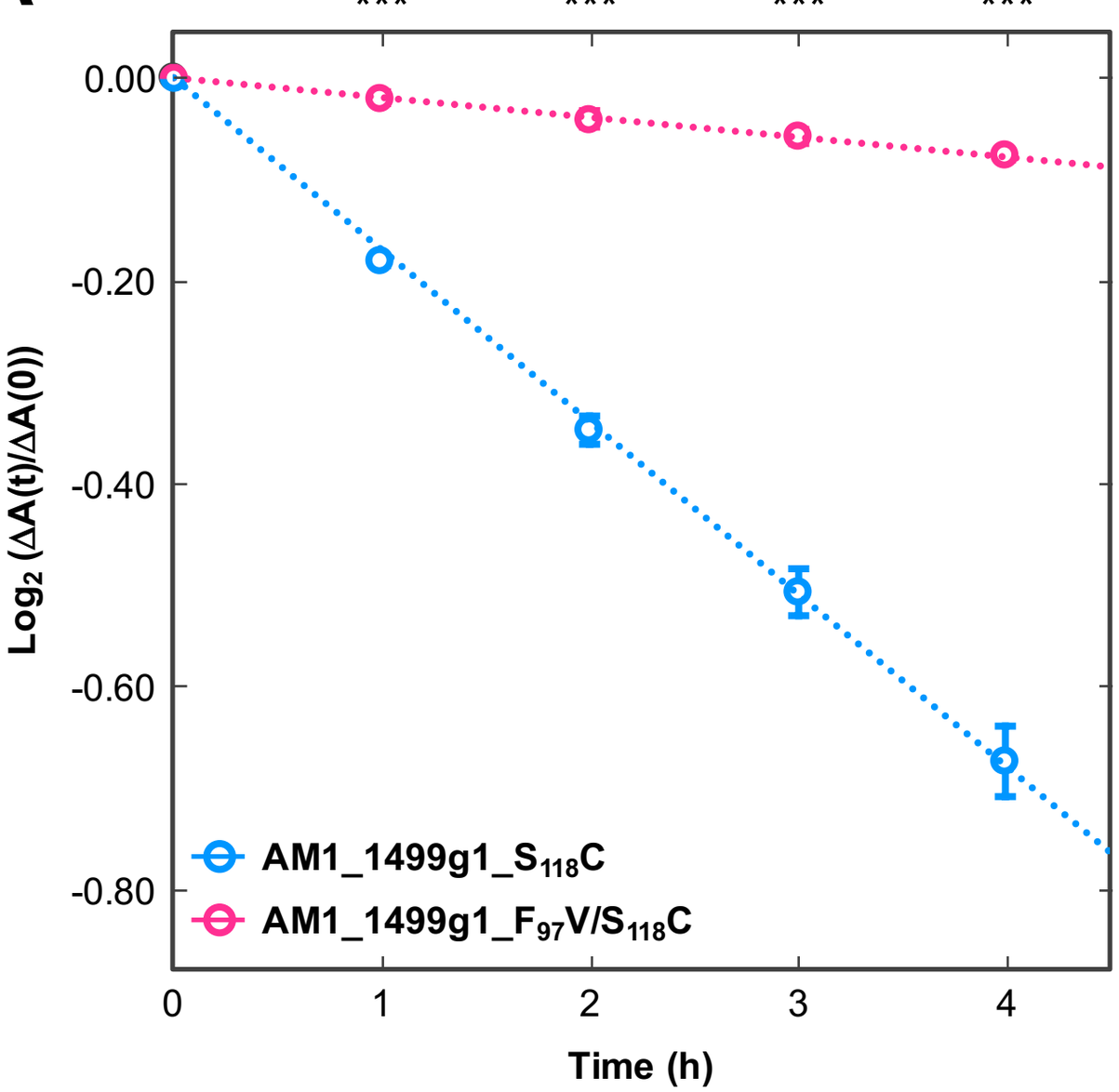
***
***
***
***
0.00
-0.20
-0.40
-0.60
-0.80
Log2 (ΔA(t)/ΔA(0))
AM1_1499g1_S118C
AM1_1499g1_F97V/S118C
0
1
2
3
4
Time (h)

C

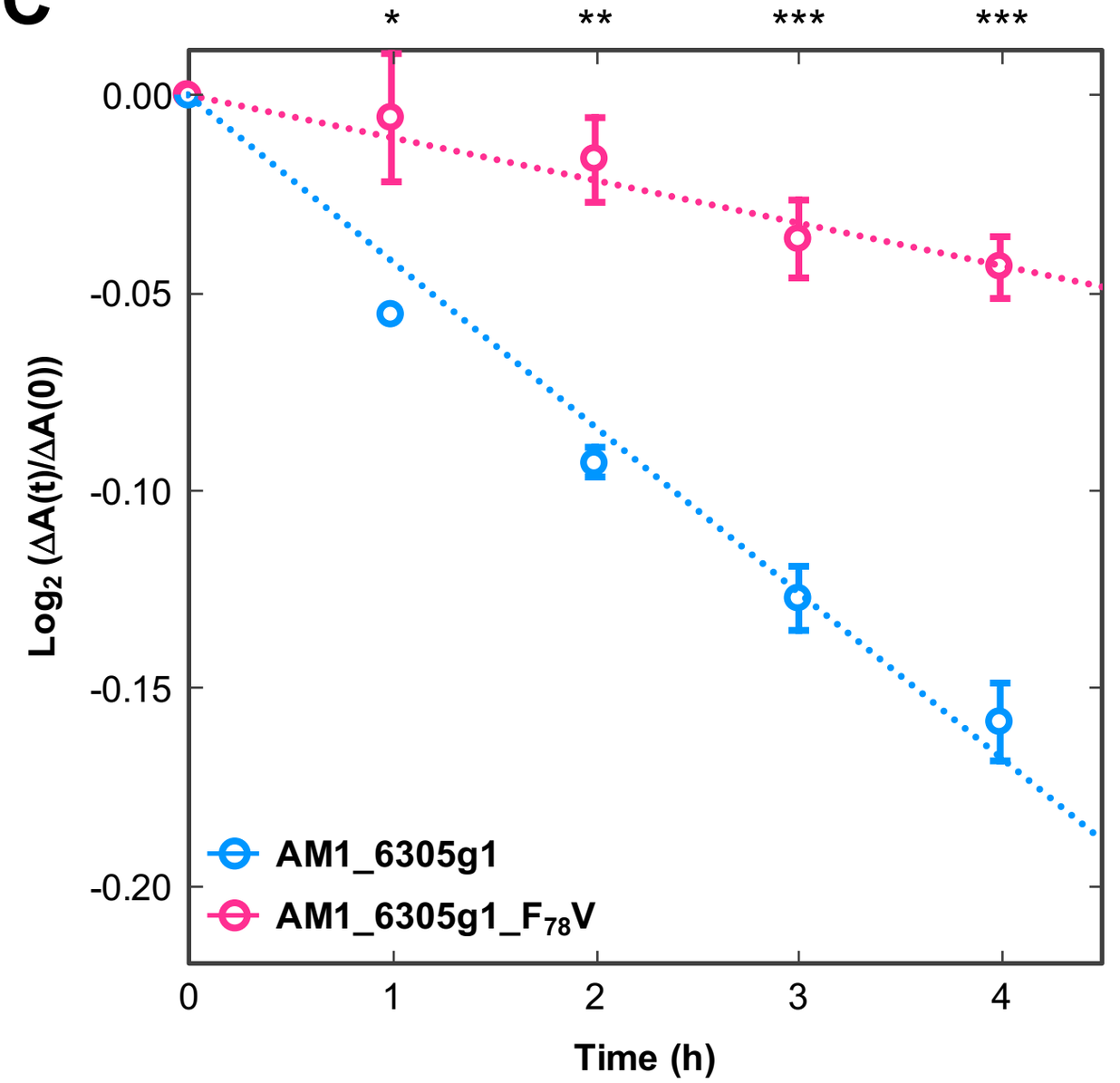
*
**
***
***
0.00
-0.05
-0.10
-0.15
-0.20
Log2 (ΔA(t)/ΔA(0))
AM1_6305g1
AM1_6305g1_F78V
0
1
2
3
4
Time (h)

B

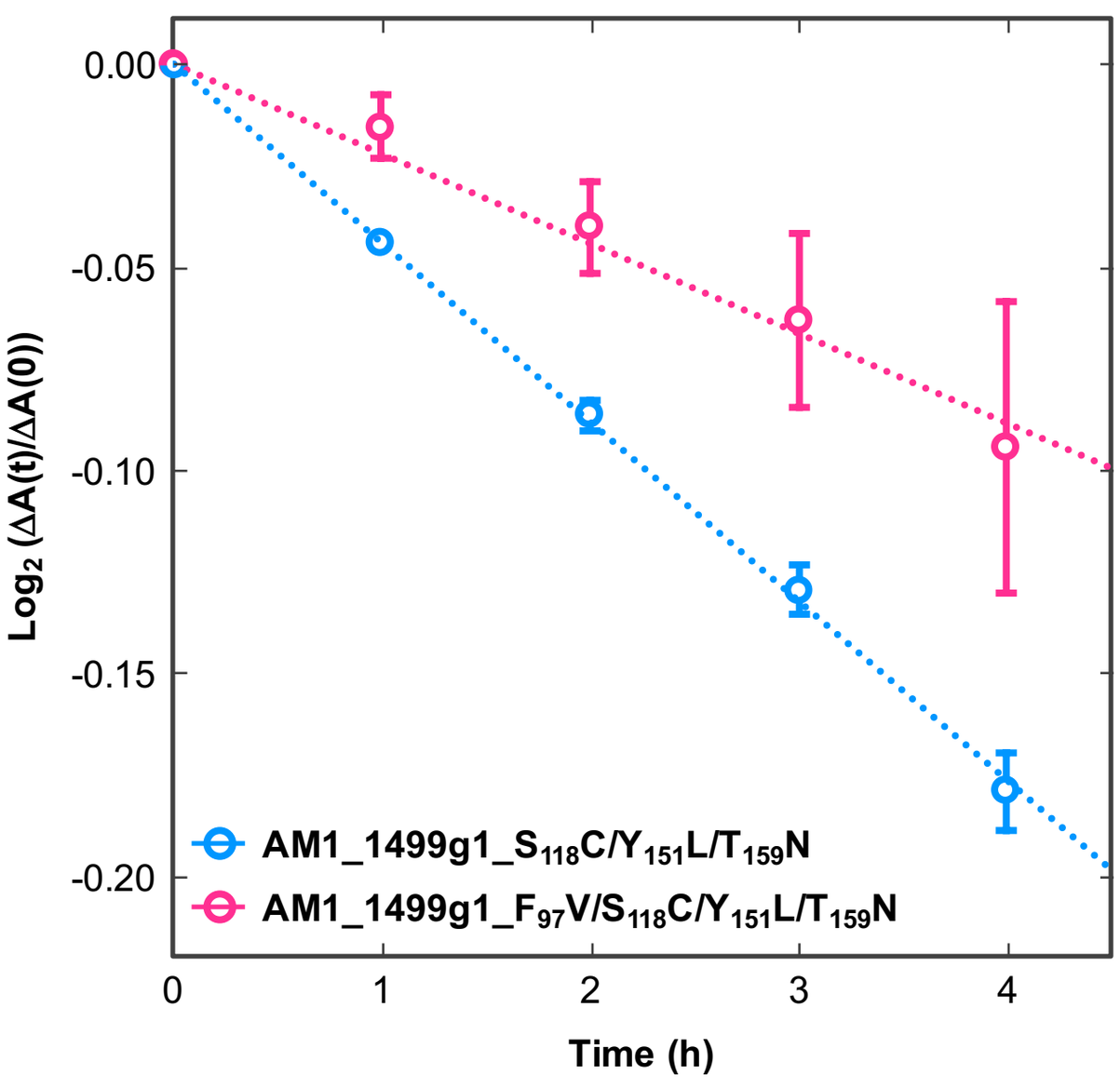
***
***
***
***
0.00
-0.05
-0.10
-0.15
-0.20
Log2 (ΔA(t)/ΔA(0))
AM1_1499g1_S118C/Y151L/T159N
AM1_1499g1_F97V/S118C/Y151L/T159N
0
1
2
3
4
Time (h)

D

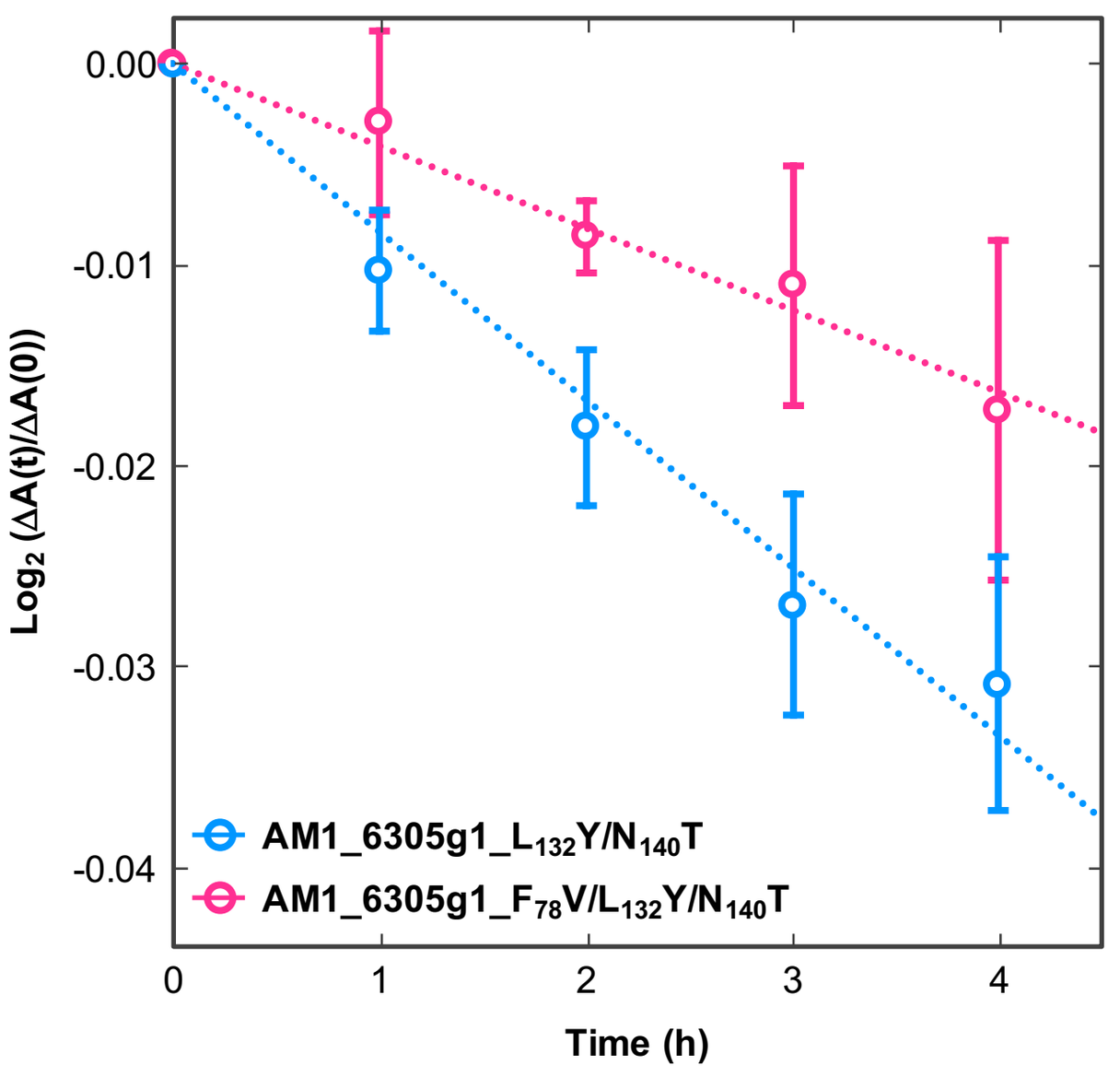
*
**
**
*
0.00
-0.01
-0.02
-0.03
-0.04
Log2 (ΔA(t)/ΔA(0))
AM1_6305g1_L132Y/N140T
AM1_6305g1_F78V/L132Y/N140T
0
1
2
3
4
Time (h)